A theory of complex patterns arising from 2D particle interactions

Theodore Kolokolnikov*, Hui Sun†, David Uminsky†, Andrea L. Bertozzi†
*Department of Mathematics and Statistics, Dalhousie University, Halifax, Canada and
†Department of Mathematics, UCLA, Los Angeles, CA 90095, USA
(Dated: August 29, 2010)

Pairwise particle interactions arise in diverse physical systems ranging from insect swarms to self-assembly of nanoparticles. This letter develops a fundamental theory for the morphology of patterns in two dimensions - which can range from ring and annular states to more complex spot patterns with N-fold symmetry. Many of these patterns have been observed in nature although a general theory has been lacking, in particular how small changes to the interaction potential can lead to large changes in self-organized state. Emergence of these patterns is explained by a stability analysis of a ring solution. This analysis leads to analytic formulae involving the interaction potential that provide detailed information about the structure of complex equilibria.

PACS numbers: 87.18.Ed, 87.10.Ed, 05.45.-a

Collective behavior of interacting systems [1] is a captivating natural phenomenon. Such systems form patterns that inspire evolutionary [2] and biological [3] questions as well as structural and physical ones. More recently, such natural behavior has inspired intelligent design of control algorithms for unmanned vehicles. Particle interaction models are extremely prevalent in the biology literature in many contexts such as insect aggregation [4], locust swarms [5]; however they also arise in other important physics applications such as self-assembly of nanoparticles [6], theory of granular gases [7], and molecular dynamics simulations of matter [8]. Regardless of whether the model is meant to describe a complex biological system such as a flock or swarm, or a basic physics application derived from first principles, a common feature of all particle interaction models is the attractive-repulsive nature of the potential. Often a 'steady state' pattern can be formulated as an extrema of a pairwise interaction energy

$$E(\vec{x}) = \sum_{i,j\neq i} P(|x_i - x_j|), \tag{1}$$

for some potential P. Typically $\vec{x}$ is the position vector of N particles so the equilibrium configuration is a minimizer of a high dimensional non-convex problem for which a fully developed predictive theory is elusive. Recent analysis [9] shows that scaling behavior of equilibrium configuration depends on the classical H-stability properties of the interaction potential [10] but does not provide a theory for morphology or symmetry class of equilibrium configuration. The last five years has seen a surge of interest in the physics literature for confining potentials which tend to yield complex equilibrium patterns. One particularly interesting question is how to infer properties of the local interactions from large scale behavior of the self-organized state [11].

The goal of this letter is to develop a general theory for prediction and classification of equilibrium patterns based on properties of the interaction potential. For simplicity, we present case studies from two different families of interaction forces $F(r) = P'(r)$ that both give spatially confined patterns: the power law force

$$F(r) = r^p - r^q; \quad 0 \le p < q \tag{2}$$

and a smoothed step discontinuity connecting $b \pm 1$:

$$F(r) = \tanh\left((1-r)a\right) + b; \quad 0 < a; \quad -1 < b < 1. \tag{3}$$

Minimizers of (1) with confining potentials can exhibit intricate structure as shown in Figure 1, for the case (3).

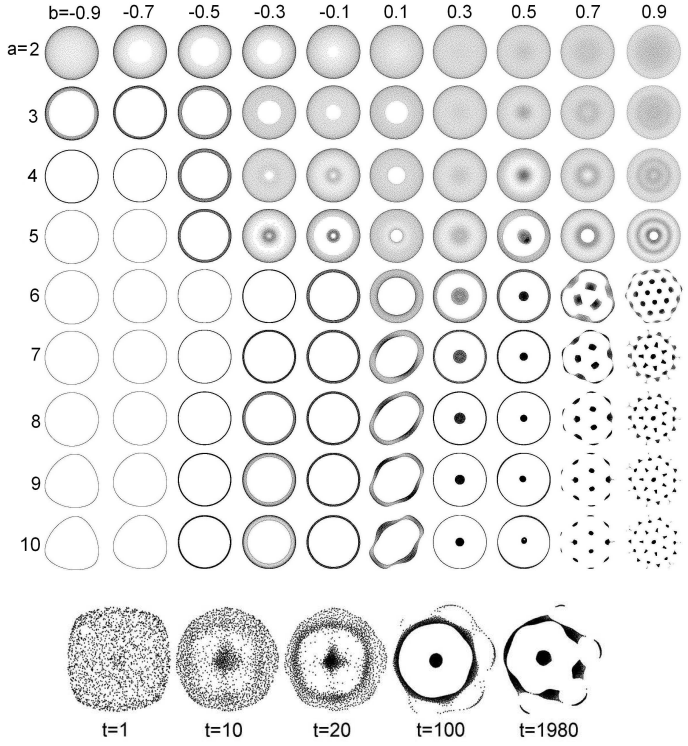

FIG. 1: Top: Minimizers of the energy (1) with force law (3). Bottom: time evolution of (4) with $a = 8$, $b = 0.67$.

Note the complex patterns ranging from rings and annuli to more complex structures exhibiting period two and three symmetry breaking to very complex 'soccer ball' like shapes. Related patterns (in particular the annuli and spotted patterns) been observed in experiments of stressed bacterial colonies [12] which have associated related nonlocal models [13]. We present a systematic methodology for predicting structures of these patterns from basic properties of the interaction potential.

Our theory is based on stability of the interaction energy under a gradient flow, although the results could be applied to more sophisticated interaction models such as those arising from the Morse potential considered in [9]. The gradient flow equations arising from (1) are

$$\frac{dx_j}{dt} = \frac{1}{N} \sum_{\substack{k=1\dots N \\ k\neq j}} F\left(|x_j - x_k|\right) \frac{x_j - x_k}{|x_j - x_k|}, \quad j = 1 \dots N. \tag{4}$$

Simulation of this system with a large number of particles results in a long time equilibrium shape. The shapes in Fig 1 are the result of a forward Euler time integration of (4) with $N = 5000$, computed to $t = 1000$ with $dt = 0.5$. Up to rotation, the results are independent of initial condition, typically taken to be random. Our theoretical approach to analyzing these patterns involves computing exact ring solutions of (4) and computing modes of instability of the ring. We find in all examples that the details of the linear instability, when it occurs, points towards specific spatial patterning of the stable equilibrium. The radius of the exact ring solution is a root of

$$I(r_0) := \int_0^{\frac{\pi}{2}} F(2r_0 \sin\theta) \sin\theta d\theta = 0, \tag{5}$$

where we assume N is large and can be approximated by a continuum. Note that any potential that has repulsion dominant at small distances and attraction dominant at large distances possesses such an exact solution. The ring is a special case of a general extrema of (1) in which the particles concentrate on a one dimensional curve. In the limit $N \to \infty$ [14], for solutions concentrated along a curve, (4) reduces to the continuum equation

$$\rho_t = -\rho \frac{< z_\alpha, z_{\alpha t} >}{|z_\alpha|^2}; \qquad z_t = K * \rho \tag{6}$$

where $z(\alpha; t)$ is a parametrization of the solution curve; $\rho(\alpha; t)$ is its density and $K * \rho =$

$$\int F\left(|z(\alpha') - z(\alpha)|\right) \frac{z(\alpha') - z(\alpha)}{|z(\alpha') - z(\alpha)|} \rho(\alpha', t) dS(\alpha'). \tag{7}$$

The formula (6) is a generalization of the classical Birkhoff-Rott equation for 2D vortex sheets [15] - applied to gradient vector fields rather than divergence free flow [14]. Linear analysis of the B-R equation describes

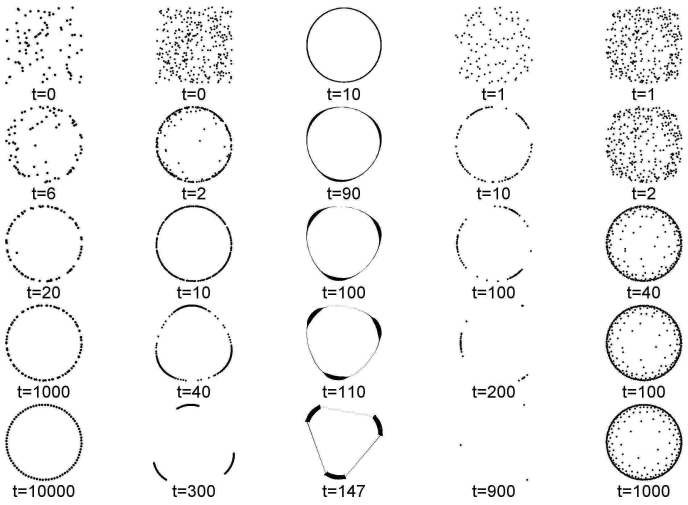

FIG. 2: Dynamics of (4). First column: $F(r) = r - r^2$, $N = 80$. Second column: $F(r) = r^{0.5} - r^6$, $N = 300$. Third column: Simluation of the continuum limit (6) with F as in the second column. Fourth column: $F(r) = r - r^{3.2}$, $N = 100$. Fifth column: $F(r) = r^{0.5} - r^{1.5}$, $N = 300$.

the classical Kelvin-Helmoltz instability in fluid dynamics and we use this as an analogy to our study of equilibrium patterns for the pairwise interaction energy (1).

Consider the perturbations of the ring of N particles of the form $x_k = r_0 \exp(2\pi i k/N)\left(1 + \exp(t\lambda)\phi_k\right)$ where $\phi_k \ll 1$. After some algebra we obtain

$$\lambda\phi_j = \frac{1}{N} \sum_{\substack{k=1..N \\ k\neq j}} G_+\left(\tfrac{\pi(k-j)}{N}\right)\left(\phi_j - \phi_k \exp\left(\tfrac{2\pi i(k-j)}{N}\right)\right) + G_-\left(\tfrac{\pi(k-j)}{N}\right)\left(\bar{\phi}_k - \bar{\phi}_j \exp\left(\tfrac{2\pi i(k-j)}{N}\right)\right),$$

where $j = 1 \dots N$, $G_\pm(\theta) = \frac{1}{2}(G_1 \pm G_2)$, and

$$G_1(\theta) = F'(2r_0 |\sin\theta|), \quad G_2(\theta) = \frac{F(2r_0 |\sin\theta|)}{2r_0 |\sin\theta|}.$$

Next we substitute $\phi_j = b_+ e^{2m\pi ij/N} + b_- e^{-2m\pi ij/N}$ where we assume that $b_\pm$ are real, and m is a strictly positive integer. This leads to a 2x2 eigenvalue problem $\lambda \begin{pmatrix} b_+ \\ b_- \end{pmatrix} = M(m) \begin{pmatrix} b_+ \\ b_- \end{pmatrix}$ where

$$M(m) := \begin{bmatrix} I_1(m) & I_2(m) \\ I_2(m) & I_1(-m) \end{bmatrix}; \quad m = 1, 2, \dots; \tag{8}$$

$$I_1(m) = \frac{4}{N} \sum_{l=1}^{N/2} G_+(\sin\frac{\pi l}{N}) \sin^2\left((m+1)\frac{\pi l}{N}\right);$$

$$I_2(m) = \frac{4}{N} \sum_{l=1}^{N/2} G_-(\sin\frac{\pi l}{N}) \left[\sin^2(\frac{\pi l}{N}) - \sin^2\left(m\frac{\pi l}{N}\right)\right].$$

Taking the limit $N \to \infty$, we obtain

$$I_1(m) = \frac{4}{\pi}\int_0^{\frac{\pi}{2}} G_+(\theta)\sin^2\left((m+1)\theta\right)d\theta; \tag{9a}$$

$$I_2(m) = \frac{4}{\pi}\int_0^{\frac{\pi}{2}} G_-(\theta)\left[\sin^2(\theta) - \sin^2\left(m\theta\right)\right]d\theta. \tag{9b}$$

The ring is linearly stable if the eigenvalues λ of (8) are non-positive for all integers $m \geq 1$; otherwise it is unstable. There are two possible types of instabilities - ones in which the ring is *long-wave unstable*, corresponding to an instability of a low order mode (small m) but stability of higher order modes. The second type corresponds to ill-posedness of the ring in which the eigenvalues are positive in the $m \to \infty$ limit and grow as m increases. In the latter case the ring completely breaks up and often forms a fully two-dimensional pattern. Such stability analysis is well-known for other types of curve evolutions involving active scalar problems – most notably the classical Kelvin-Helmholtz instability (ill-posedness) of the vortex sheet for the 2D Euler equations [15].

Figure 2 shows evolutionary behavior of (4) with force law (2). In the first column, the equilibrium solution is a stable ring. Random initial conditions quickly converge to a ring shape ($t = 20$); this is followed by slow dynamics along the ring until equilibrium is achieved by $t = 10000$. In column 2 a mode $m = 3$ instability is triggered on a slower timescale than the initial collapse to a ring shape. The final steady-state is a triangular shape, which retains some of the features of the initial instability. Column three is the direct numerical simulation of the continuum equations (6) with the same parameters as Column two. The thickness represents the variable density ρ. In the fourth column, the ring appears as a transient state, but final equilibrium consists of just three points. Column five shows another type of instability, which corresponds to very high modes m; the ring solution is not only linearly unstable but also linearly ill-posed; the resulting swarm has a two-dimensional shape.

For interaction force (2), and with $p = 1, q = 2$ we have

$$\text{tr } M(m) = -\frac{\left(4m^4 - m^2 - 9\right)}{(4m^2-1)(4m^2-9)} < 0, \quad m = 2, 3, \ldots$$

$$\det M(m) = \frac{3m^2(2m^2+1)}{(4m^2-9)(4m^2-1)^2} > 0, \quad m = 2, 3, \ldots$$

This proves that the **ring pattern corresponding to $F(r) = r - r^2$ is locally stable**. Moreover, for large m, the two eigenvalues are $\lambda \sim -\frac{1}{4}$ and $\lambda \sim -\frac{3}{8m^2} \to 0$ as $m \to \infty$. The presence of small eigenvalues implies the existence of slow dynamics near the ring equilibrium. Further analysis shows that the eigenvector corresponding to the small eigenvalue and large m is nearly tangential to the circle; the other eigenvector is nearly perpendicular. The corresponding two-time dynamics are also clearly visible in simulations (Figure 2, column 1).

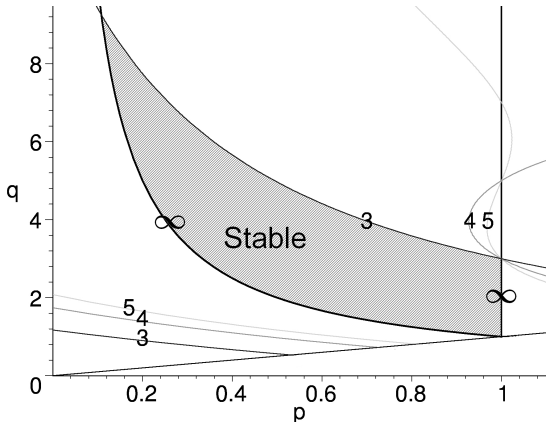

FIG. 3: Stability diagram for (2). The curves shown correspond to the boundaries of the stability $\det(M(m)) = 0$, with $m = 3, 4, 5$ and $m = \infty$, as indicated. The line $p = q$ is also drawn. Crossing any of the curves destabilizes the ring. The intersection of $m = \infty$ and $m = 3$ boundaries is at $p = 0.10779,\ q = 9.277102$.

In general, if $F(0) > 0$ and F is C^2, the asymptotics for large m yield

$$I_1(m) \sim I_1(-m) \sim \frac{F(0)}{2\pi r_0}\ln m + O(1) \text{ as } m \to \infty.$$

This shows that trace $M(m) > 0$ for sufficiently large m. It follows that the necessary condition for well-posedness of a ring is that $F(0) = 0$. If in addition, F is C^4, then using integration by parts we obtain

$$\text{tr } M(m) \sim \frac{2}{\pi}\int_0^{\pi/2}\left(\tfrac{F(2r_0\sin\theta)}{2r_0\sin\theta} - F'(2r_0\sin\theta)\right)d\theta + O\left(\tfrac{1}{m^2}\right);$$

$$\det(M(m)) \sim \text{tr } M(m)\frac{F''(0)r_0}{m^2} + O\left(\frac{1}{m^4}\right).$$

In summary, **if $F(r)$ is C^4 on $[0, 2r_0]$, then the necessary and sufficient conditions for well-posedness of a ring are:**

$$F(0) = 0, \quad F''(0) < 0 \text{ and} \tag{10}$$

$$\int_0^{\pi/2}\left(\frac{F(2r_0\sin\theta)}{2r_0\sin\theta} - F'(2r_0\sin\theta)\right)d\theta < 0. \tag{11}$$

In particular, **the ring solution for the force (3) is always ill-posed,** since $F(0) > 0$. Another general result is if F is odd and C^∞ on $[0, 2r_0]$. In that case, one can show that $\det(M(m)) = 0$ for all m; the ring then has infinitely many zero eigenvalues. This observation may be relevant for the Kuramoto model $F(r) = \sin(r)$ [16].

For the force of type (2) with $0 < p < q$, the asymptotics of the mode $m = \infty$ can be computed in terms of Gamma functions. It can be shown that the mode $m = \infty$ is stable if and only if $pq > 1$ and $p < 1$. In

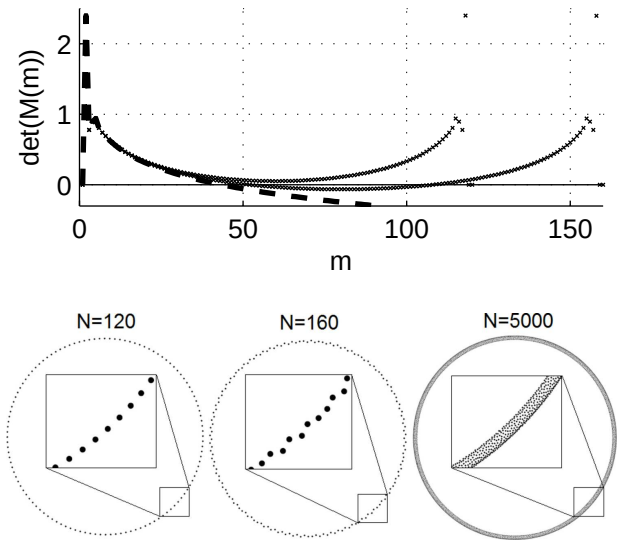

FIG. 4: Stability of discrete vs. continuous system for $F(r) = \tanh(4(1-r))-0.5$. Top: $\det(M(m))$. Dashed line corresponds to continuum eq. (10) and crosses to discrete eq. (9) with $N = 120, 160$. Instability occurs iff $\det(M(m)) < 0$. Bottom: steady states of discrete dynamics with N as indicated; inserts show the blowup of the ring structure.

addition, the low modes $m = 2, 3, 4, \ldots$ may also become unstable, see Figure 3. The dominant unstable mode corresponds to $m = 3$, which bounds the stability region from above. This boundary is given implicitly by

$$\begin{aligned} 0 &= 723 - 594(p+q) - 27(p^2+q^2) - 431pq \\ &+ 106\left(pq^2+p^2q\right) + 19\left(p^3q+pq^3\right) \\ &+ 10\left(p^3q^2+p^2q^3\right) + 6\left(p^3+q^3\right) + p^3q^3 \end{aligned}$$

and is shown in Figure 3. Similarly, the stability boundary for $m = 2$ mode is given by $0 = 7 + 38(p+q) + 12pq + 3(p^2+q^2) + 2\left(pq^2+p^2q\right) - p^2q^2$; this boundary happens to lie well outside the area shown in Figure 3. The stability boundaries for modes $m = 4, 5, \ldots$ are also expressed in terms of higher order polynomials in p, q.

Even if (4) is ill-posed in the *continuous* limit $N \to \infty$, the ring of *discrete* particles (4) may be stable with a relatively large N as in Figure 4. Note the slight instability for $N = 160$ but stability when $N = 120$. The continuous limit is well approximated with $N = 5000$; the resulting steady state appears to be a thin annulus, whose inner and outer radius are approximately r_0 given by (5).

Many open questions remain. In a recent work [17], the authors studied the collapse of N particles into K points in one dimension, each point having roughly N/K particles. When $F(r) = r - r^s$, they showed that N particles collapse to two points when $s \geq 2$; no collapse occurs when $1 < s < 2$. In contrast, our analysis of this problem in 2D shows that the ring is stable for all $1 < s < 3$. Numerics show that the ring collapses into three points when $s > 3$.

Another open question is to study the annulus and spot-type solutions, such as shown in Figure 1. These tend to arise in the limit where $F(r)$ has a sharp transition from repulsive to attractive regime. Unlike the ring solutions discussed above or point solutions of [17], the requirement $F(0) = 0$ is not necessary.

Numerics suggest that random initial conditions tend to converge to ring solutions, whenever the ring is stable. Global stability of the ring remains an open question.

Acknowledgements: T.K. is supported by NSERC grant 47050. D.U. is supported by NSF grant DMS-0902792 and a UC Presidents Fellowship. A.B. and H.S. are supported by NSF grants DMS-0907931 and EFRI-1024765 and ONR grant N000141010641. We thank Andrew Bernoff for helpful comments.

[1] S. Camazine *et al. Self Organization in Biological Systems* (Princeton Univ. Press, Princeton, 2003); I. Prigogine, *Order out of Chaos* (Bantam, New York, 1984).

[2] J. K. Parrish and L. Edelstein-Keshet, Science 284, 99 (1999); S. A. Kaufmann, *The Origins of Order: Self-Organization and Selection in Evolution* (Oxford University Press, New York, 1933).

[3] I. D. Couzin, J. Krauss, N. R. Franks, and S. A. Levin, Nature (London) **433**, 513 (2005); I. Reidel, K. Kruse, and J. Howard, Science **309**, 300 (2005); G. Flierl, D. Grünbaum, S. A. Levin, and D. Olson, J. Theor. Biol. **196**, 397 (1999).

[4] A. Mogilner, L. Edelstein-Keshet, L. Bent, A. Spiros, J. Math. Biol. 47, 353 (2003); L. Edelstein-Keshet, J. Watmough, D. Grunbaum, J. Math. Biol. 36, 515 (1998).

[5] C.M. Topaz, A.J. Bernoff, S. Logan, and W. Toolson, Eur. Phys. J. Special Topics 157, 93–109 (2008); C.M. Topaz, A.L. Bertozzi, and M.A. Lewis, Bull. Math. Biol. 68:1601–1623 (2006); A.J. Leverentz, C.M. Topaz and A.J. Bernoff, SIAM J. Appl. Dyn. Sys. 8(3),880–908 (2009).

[6] D. D. Holm and V. Putkaradze, Phys. Rev. Lett. 95, 226106 (2005).

[7] N. V. Brilliantov and T. Pöschel, in *Granular Gases*, vol 564, Lecture Notes in Physics, Springer-Verlag, Berlin, 2000, p. 100; R. Ramirez, T. Pöschel, N. V. Brlliantov, and and T. Schwager, Phys. Rev. E, 60, 4465 (1999); G. Toscani RAIRO Modél Math. Anal. Numér. 34, 1277 (2000).

[8] J. M. Haile *Molecular Dynamics Simulation: Elementary Methods* (John Wiley and Sons, Inc., New York, 1992).

[9] M.R. D'Orsogna, Y.L. Chuang, A.L. Bertozzi, and L. Chayes, Phys. Rev. Lett., 96 (2006), paper 104302; Y.-L. Chuang, M. R. D'Orsogna, D. Marthaler, A. L. Bertozzi, and L. Chayes, Physica D, 232, 33-47, 2007.

[10] D. Ruelle, Statistical Mechanics (Benjamin, New York), 1969.

[11] R. Lukeman, Y.-X. Li, and L. Edelstein-Keshet, PNAS **107**(28), 12576 (2010).

[12] L. Tsimring, H. Levine, I. Aranson, E. Ben-Jacob, I.

Cohen, O. Shechet, and W. Reynolds, PRL 75(9) 1859 (1995); A. M. Deprato, A. Samadani, A. Kudrolli, and L. S. Tsimring, PRL 87(15) 158102.

[13] E. F. Keller and L.A. Segel, J. Theor. Biol., 30:225-234(1971); M.P. Brenner, P. Constantin, L. P. Kadanoff, A. Shenkel and S.C. Venkataramani, Nonlinearity 12:4, 1071-1098(1999); MP Brenner, LS Levitov, EO Budrene, Biophys. J. 74:4, 1677-1693 (1998).

[14] H. Sun, D. Uminsky, A. Bertozzi, preprint 2010.

[15] R. Krasny, J. Fluid Mech. 167, 65–93 (1986)

[16] S.H. Strogatz, Physica D 143 (2000) 1–20.

[17] K. Fellner and G. Raoul, to appear, Math. Models Methods Appl. Sci.